

LASER: Neuro-Symbolic Learning of Semantic Video Representations

Jiani Huang^{1,2}, Ziyang Li², David Jacobs¹, Mayur Naik², and Ser-Nam Lim¹

¹Meta AI

{jiani.h, dwjacobs, sernamlim}@meta.com

²University of Pennsylvania

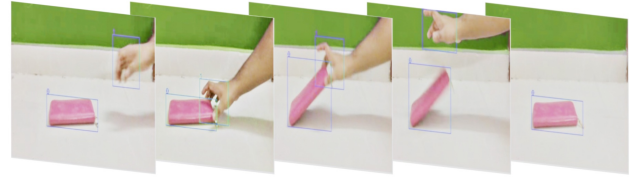
{jiani.h, liby99, mhnaik}@seas.upenn.edu

Abstract

Modern AI applications involving video, such as video-text alignment, video search, and video captioning, benefit from a fine-grained understanding of video semantics. Existing approaches for video understanding are either data-hungry and need low-level annotation, or are based on general embeddings that are uninterpretable and can miss important details. We propose LASER, a neuro-symbolic approach that learns semantic video representations by leveraging logic specifications that can capture rich spatial and temporal properties in video data. In particular, we formulate the problem in terms of alignment between raw videos and specifications. The alignment process efficiently trains low-level perception models to extract a fine-grained video representation that conforms to the desired high-level specification. Our pipeline can be trained end-to-end and can incorporate contrastive and semantic loss functions derived from specifications. We evaluate our method on two datasets with rich spatial and temporal specifications: 20BN-Something-Something and MUGEN. We demonstrate that our method not only learns fine-grained video semantics but also outperforms existing baselines on downstream tasks such as video retrieval.

1. Introduction

Understanding the semantics of video data has gained prominence due to a wide range of real-world applications such as video search, text-video retrieval, video question answering, video segmentation, and video captioning. In particular, there are two important aspects of video semantics: *spatial semantics* and *temporal semantics*. Spatial semantics concern the entities in the video, their individual attributes, and their semantic relationships. For example, as shown in Figure 1, “a sponge is originally on the table”



Video Caption: lift and drop a **sponge**

Fine-Grained Video Caption

A **sponge** is originally on the **table**;
after being lifted by a **hand**, it drops back onto the **table**.

Figure 1: A video of a hand first lifting then dropping a sponge. The fine-grained video semantics is captured in a spatio-temporal specification written in natural language.

specifies two entities, “sponge” and “table”, connected by the relation “on”. Temporal semantics, on the other hand, capture actions and properties evolving through time. For instance, “after being lifted by a hand, the sponge drops back onto the table” describes two temporally consecutive actions “lift” and “drop”.

Significant progress has been made in capturing each aspect of semantics. A well-known representation of spatial semantics is a *Scene Graph* [23, 27], extracted by scene graph generation (SGG) procedures [45]. Likewise, temporal semantics is typically specified by an *action sequence* that describes a series of events. To explicitly learn combined spatial and temporal semantics, *Spatio-Temporal Scene Graph* (ST-SG) [39, 45] has been proposed to represent entity relations throughout a video. However, due to its complexity, the low-level annotation is hard to obtain, and the problem of generating such graphs remains open.

In this paper, we propose a method called LASER¹ to explicitly learn both spatial and temporal semantics with

¹Learning to Align for Spatio-tEmporal Representations.

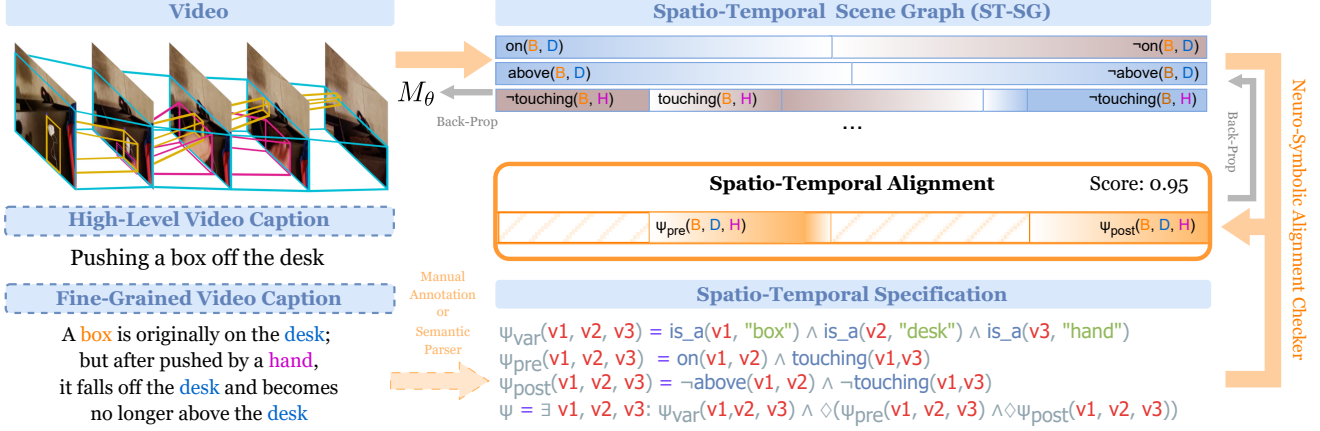


Figure 2: A 20BN example showing the end-to-end learning pipeline. The spatio-temporal specification describes a temporal ordering of a pre-condition ψ_{pre} and a post-condition ψ_{post} , while each condition details requirements for entity relationships.

only weak supervision. One of the core challenges for weak supervision is the format of its representation. LASER uses an extended *Linear Temporal Logic* (LTL) [34] to provide a logic specification for video. LTL is a powerful specification language for describing temporal properties, such as the order of events. LTL strictly subsumes action sequences commonly seen in video-action alignment tasks, while capturing additional temporal nuances such as “until” and “finally”. Moreover, it allows the expression of common-sense constraints, such as “if one drops the sponge, it leaves one’s hand.” Finally, combined with relational predicates over entities, it can specify the spatial semantics of video.

In this work, we assume that the logic specification is given for each video. While such specifications are usually unavailable in existing datasets, they can be extracted from natural language captions or mined from common-sense knowledge bases. The challenge then is how to systematically learn the video semantics from the weak supervision provided by the specification. LASER adopts the neuro-symbolic learning paradigm [19, 26, 29, 40], which is well-known for providing weak supervision via logical reasoning. In particular, we design an LTL specification checker based on Scallop [19], a general-purpose neuro-symbolic engine. The checker computes an *alignment score* between a pair of predicted video semantics and an LTL specification. Through end-to-end differentiable reasoning, the video semantics can then be learnt by back-propagating the alignment loss for stochastic gradient descent. We show that this framework is capable of deriving semantic loss through temporal constraints, as well as contrastive loss through matching and non-matching video-specification pairs.

We evaluate our method on two datasets, 20BN-Something-Something [14] and MUGEN [16]. The LTL specifications collected from these two datasets exhibit diverse patterns, including action sequences, action pre-

and post-conditions, evolving entity relationships, and common-sense temporal constraints. We qualitatively illustrate that our method learns high-quality video semantic representations, outperforming existing baselines. Moreover, we demonstrate that our method can be used in downstream tasks such as text-video retrieval, and provides benefits such as explainability and better accuracy.

We summarize the main contributions of this work as follows: 1) we propose a novel semantic video representation learning framework with linear temporal logic specifications; 2) we design a loss function combining alignment loss, temporal constraint semantic loss, and contrastive loss for specification-guided learning; 3) we perform evaluation on two video understanding datasets, demonstrating superior performance on video semantics extraction and downstream tasks such as video retrieval.

2. Related Work

Joint Visual-Textual Learning is crucial in video understanding and has a wide range of downstream applications. Current works have succeeded in learning visual representations using large-scale paired visual-textual data through contrastive learning in both image-text [20, 35] and video-text representation [25, 32, 42] learning. A downstream application of the joint visual-textual learning task is visual-text retrieval, which aims to learn a multi-modal encoder to project both modalities onto a joint embedding space and compute a similarity score between the visual and textual data [3, 15, 24, 28, 35].

Weakly-Supervised Visual-Textual Alignment aims to synchronize an ordered textual input with a video based on its time span given just video-level labels. The main challenge in this task lies in how to train without having access to the specific time boundaries corresponding to the text. To mitigate this issue, an iterative process is usually adopted to

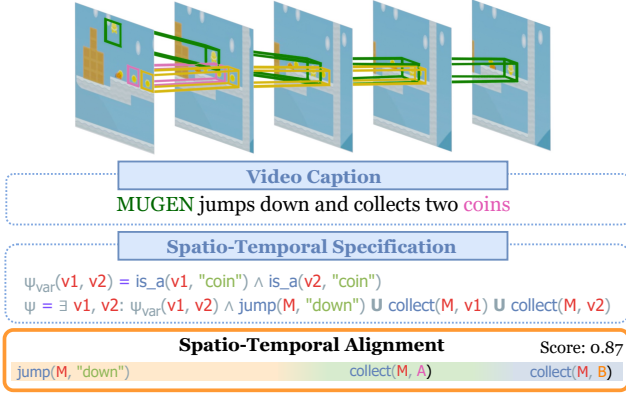


Figure 3: One example from the MUGEN dataset whose specification is a consecutive sequence of actions.

first estimate and then refine the low-level time boundaries from the video-level labels. Such approaches include both dynamic time warping [6, 10, 12, 36] and soft nearest neighbor [13, 15]. There are also works incorporating temporal logic into the learning process as a semantic loss [43].

Neuro-Symbolic Methods [17] are known for their decoupling of complex learning systems into perceptual and reasoning systems. There are a wide range of neuro-symbolic approaches solving individual computer vision tasks, such as visual reasoning [2, 7], visual-question-answering (VQA) [19, 30], and video action aligning [6, 18]. Due to the recent surge of general-purpose neuro-symbolic programming systems [19, 29, 40], there is growing interest in scaling point-solutions into more general and complex systems. LASER utilizes one such general-purpose neuro-symbolic programming system, Scallop [19], for extracting temporal and spatial semantics from videos.

3. Illustrative Overview

We illustrate our approach using two examples adapted from the 20BN-Something-Something (20BN) dataset [14] and the MUGEN dataset [16] (Figures 2 and 3). The 20BN dataset contains real-life short videos involving a human performing simple actions, such as “push”, “move-towards”, and “lift”, on other objects. The MUGEN dataset contains short gameplay footage of a 2D platform game *CoinRun*. In the video game, the player character MUGEN can walk, jump, collect coins, and kill enemies.

Our model takes two inputs for the task of learning a fine-grained semantic video representation. The first is the video. For simplicity, we assume the main entities in the video are already detected and bounding-boxes are extracted. The second is a description of the entities and events happening in the video, usually obtained from natural language video captions. The goal of the task is to learn a fine-grained semantic video representation, in this case

the *spatio-temporal scene graph* (ST-SG), capturing entities, their relationships, events, and evolving properties.

One long-standing challenge is capturing structured semantics from the natural language (NL) captions. While being easier to collect as data, NL captions vary significantly in terms of the level of details. For example, Figure 2 shows two different captions, one describing a single high-level action, and the other specifying evolving properties of objects in the video. Figure 3 shows another caption which describes a sequence of actions. In this work, instead of directly processing NL captions, we propose to employ a spatio-temporal specification language. This language is based on the formalism of linear temporal logic (LTL), and can precisely capture the nuance of temporal relations. Note that one can train, fine-tune, or learn-in-context a semantic parser for converting NL captions. We assume the specification is given for each datapoint and can be used for training. We elucidate how we obtain such specifications for our presented datasets in §6.

Figure 2 shows one spatio-temporal specification describing the pre- and post-condition of a single high-level action “push”. Before a box is pushed off the desk, it must be on the desk ($\text{on}(v1, v2)$), and a hand is touching it ($\text{touching}(v1, v3)$). After it is pushed off the desk, it must be under the desk ($\neg \text{above}(v1, v2)$). In the specification, the pre- and post-conditions are connected using several \Diamond (finally) operators. This specification means, the post-condition has to happen after the pre-condition, but the two states are not required to be consecutive.

Figure 3 shows another specification connecting three events “jump”, “collect”, and “collect” together using the \cup (until) operator. This suggests that the three events are likely consecutive. Different from traditional sequence of actions [6, 18], the events here are relational predicates connecting entities and possibly properties. For example, $\text{jump}(M, \text{'down'})$ specifies that the actor of jump is (M)UGEN, and that the direction of jump is “down”.

Despite expressing diverse semantics, both specifications can be uniformly represented under our LTL based formalism. The next question is how to learn the underlying ST-SG from video and specifications. In this work, we frame it as a weakly-supervised specification alignment problem, illustrated in Figure 2. That is, the ST-SG extracted from video should align with (i.e., satisfy) the corresponding logic specification. We design a neuro-symbolic alignment checker to compute an alignment score, i.e., the probability of alignment. During training, our approach learns to extract an ST-SG such that it maximizes the alignment score between a corresponding pair of video and specification. With additional semantic and contrastive loss, we show that our method can effectively generate an ST-SG that conforms to the specification.

4. Background

Neuro-Symbolic Methods [26, 30] seek to integrate low level perception and high level logical reasoning in complex learning systems. A typical neuro-symbolic model consists of a separate neural perception model (M_θ) and logical reasoning component (P). Given an input-output pair (x, y) , M_θ processes unstructured data x , such as video or image, and predicts a structured representation \hat{r} . Subsequently, logic program P takes in \hat{r} and deduces the predicted result \hat{y} . LASER employs Scallop [19] as the back-end neuro-symbolic reasoning engine. In this case, the structured representation is a probabilistic relational database [9], which we elaborate below. Logic programs defined in Scallop are differentiable and hence the perceptual model M_θ can be trained in an end-to-end and weakly supervised fashion, i.e., no supervision is provided on intermediate representation \hat{r} . Existing works [4, 44] show that such logic programs P can encode deductive rules, common sense knowledge, specifications, and semantic loss.

Probabilistic Relational Database. Our back-end neuro-symbolic framework, Scallop [19], uses a probabilistic relational database as the intermediate symbolic representation. Each entry in the database is called a *fact*, denoted $p :: a(c_1, \dots, c_n)$. Here, a is an n -ary relational predicate, while c_1, \dots, c_n are constant arguments to the predicate. p is the probability of this fact being true, typically predicted by neural networks. For a fact that is always true (i.e., non-probabilistic), the probability p is automatically set to 1, and we might omit writing “1 ::” for simplicity. In this work, we use the above notation to represent the structured video representation. For example, we use the fact $0.95 :: \text{walk}(3, \text{M}, \text{Right})$ to represent that the vision network predicts “the MUGEN is walking to the right in the 3rd clip of the video” with a probability of 0.95.

Differentiable Logic Programming and Datalog. Many neuro-symbolic frameworks [19, 29, 40] are based on logic programming languages that support reasoning over probabilistic relational databases. Scallop, in particular, is based on the Datalog language. A Datalog program consists of a set of deductive *horn rules*, which can be applied to the database to derive new facts. When executing such a program, Scallop’s reasoning engine iteratively applies all rules on the input database until no new fact is derived. Notice that the derived facts will be associated with probabilities along with the gradients with respect to the input probabilities. This differentiable probabilistic reasoning is done through Scallop’s underlying provenance system. In this work, we rely on the Datalog language to define the temporal reasoning module for video-specification alignment.

Linear Temporal Logic. Linear Temporal Logic (LTL) [34] is a formal logic system extending propositional logic with concepts about time. It is commonly used for formally describing temporal events, with applications in verification

$$\begin{array}{ll} \text{(Specification)} & \psi ::= \exists v_1, \dots, v_k : \varphi \\ \text{(Formula)} & \varphi ::= \alpha \mid \psi_1 \wedge \psi_2 \mid \neg \psi \\ & \mid \Box \psi \mid \Diamond \psi \mid \bigcirc \psi \mid \psi_1 \mathbf{U} \psi_2 \end{array}$$

Figure 4: The formal syntax of our LTL system.

of software [5, 22] and control systems [11, 37]. In this paper, we use LTL as a framework for specifying events and their temporal relationships occurring in a video. Note that LTL is a fragment of the more general *Computation Tree Logic* (CTL*), which can model time in a tree-like structure where the future is not yet determined. Since this work is centered around pre-recorded and finite-length videos, LTL is sufficient for providing temporal specification.

Our LTL system (Figure 4) starts from the specification ψ which existentially quantifies variables in an LTL formula. The formula φ is inductively defined, with basic elements as relational atoms α of the form $a(t_1, \dots, t_n)$. Note that each term t_i can be a quantified variable to be later grounded into a concrete entity. From here, φ can be constructed using basic propositional logic components \wedge (and), \vee (or), and \neg (not). The system additionally includes temporal unary operators \Box (always), \Diamond (finally), \bigcirc (next), and a binary operator \mathbf{U} (until) [1]. For example, the description “MUGEN starts by climbing the stairs; immediately after that, it walks to the right” can be represented as an LTL formula

$$\psi = \text{climb}(\text{M}, _) \mathbf{U} \text{walk}(\text{M}, \text{right}). \quad (1)$$

Note that an argument to the predicate `climb` is a wildcard ($_$), since we do not specify whether it is climbing up or down. This formula might seem too strict since it requires the two events to be consecutive. To make the specification more natural, one can change the above formula to “ $\Diamond(\text{climb}(\text{M}, _) \wedge \Diamond \text{walk}(\text{M}, \text{Right}))$ ”. Here, the two events, `climb` and `walk`, need to happen in chronological order but are not required to be consecutive.

LTL formulas can be evaluated against a concrete finite event sequence for *satisfaction*, or *alignment*. Given a space of all possible events Σ , a size n event sequence $s : \{1 \dots n\} \rightarrow 2^\Sigma$ is a mapping from a time-step $i \in 1 \dots n$ to a set of events happening at that time-step. We write $s \models \psi$ iff the sequence s satisfies an LTL formula ψ . For example, given the formula ψ from Eqn. 1, we have $[c, c, w, w] \models \psi$ and $[c, c, c, c] \not\models \psi$ ². This computational problem can be expressed in Datalog, the logic programming language supported by Scallop.

5. Methodology

We begin by presenting the high-level problem definition. We are given a dataset \mathcal{D} of video-specification pairs (X, ψ) , where $X = [x_1, \dots, x_n]$ is a video containing n

²We use `c` and `w` to denote singleton sets of events containing only `climb(M, Up)` and `walk(M, Right)`.

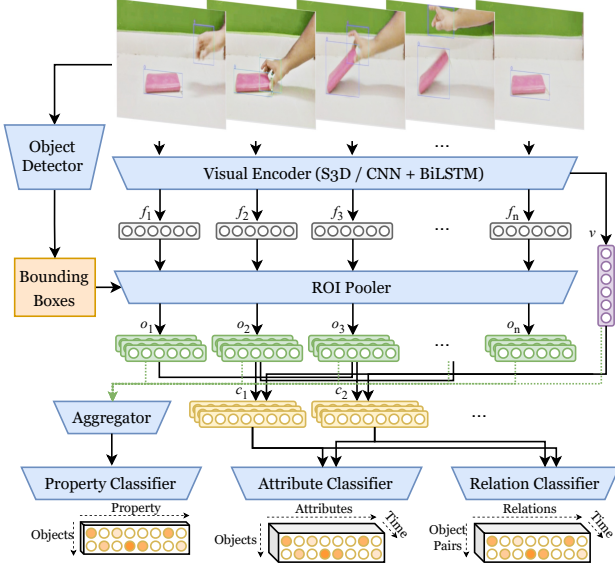


Figure 5: Model architecture of M_θ for extracting ST-SG.

frames, and ψ is a spatio-temporal specification using LTL. We wish to learn a neural model M_θ which extracts a fine-grained video representation $\hat{\mathbf{r}} = M_\theta(X)$ that conforms to the corresponding temporal specification ψ . During training time, given a loss function \mathcal{L} , we aim to minimize the following main objective:

$$J(\theta) = \frac{1}{|\mathcal{D}|} \sum_{(X, \psi) \in \mathcal{D}} \mathcal{L}(\Pr(M_\theta(X) \models \psi), 1), \quad (2)$$

where $\Pr(\hat{\mathbf{r}} \models \psi)$ is the alignment score (probability of alignment) computed by our spatio-temporal alignment checker. In this section, we first describe our video semantics representation using a probabilistic relational database (§5.1). Then, we present the alignment checker in §5.2. Lastly in §5.3, we present the overall learning pipeline and the other loss functions for the robustness of our method.

5.1. Video to Probabilistic Relational Database

The neural perception model M_θ , parametrized by θ , converts pixel-based raw video data X into a structured ST-SG, which is encoded as a probabilistic relational database $\hat{\mathbf{r}} = M_\theta(X)$. The general architecture of M_θ is illustrated in Figure 5. At a high level, the model has three classification heads extracting three types of probabilistic information. Note that we assume that a relational schema is pre-defined and given for each task, meaning that the dimensions of classification heads are known beforehand. By associating the classification outputs with explicit relational symbols, we then construct the database $\hat{\mathbf{r}}$. Here are the three types of probabilistic facts:

1. Static properties. E.g., $0.95 :: \text{is-bendable}(e)$ represents “the entity e is bendable at all times”.

$\mathbf{r} \models \psi$	iff	$\psi = \exists v_1, \dots, v_k : \varphi$ and there exists $\Gamma : V \mapsto E$, $\langle \mathbf{r}, [1 : m], \Gamma \rangle \models \varphi$
$\langle \mathbf{r}, [s : t], \Gamma \rangle \models \alpha$	iff	$\forall i \in s \dots t$, $\text{substitute}_\Gamma(\alpha) \in \mathbf{r}[i]$
$\langle \mathbf{r}, [s : t], \Gamma \rangle \models \varphi_1 \wedge \varphi_2$	iff	$\langle \mathbf{r}, [s : t], \Gamma \rangle \models \varphi_1$ and $\langle \mathbf{r}, [s : t], \Gamma \rangle \models \varphi_2$
$\langle \mathbf{r}, [s : t], \Gamma \rangle \models \neg \varphi$	iff	$\langle \mathbf{r}, [s : t], \Gamma \rangle \not\models \varphi$
$\langle \mathbf{r}, [s : t], \Gamma \rangle \models \bigcirc \varphi$	iff	$\langle \mathbf{r}, [s + 1 : t], \Gamma \rangle \models \varphi$
$\langle \mathbf{r}, [s : t], \Gamma \rangle \models \Box \varphi$	iff	$\forall i \in s \dots t$, $\langle \mathbf{r}, [i : i], \Gamma \rangle \models \varphi$
$\langle \mathbf{r}, [s : t], \Gamma \rangle \models \Diamond \varphi$	iff	$\exists i \in s \dots t$, $\langle \mathbf{r}, [i : i], \Gamma \rangle \models \varphi$
$\langle \mathbf{r}, [s : t], \Gamma \rangle \models \varphi_1 \mathbf{U} \varphi_2$	iff	$\exists i, s < i < t$, $\langle \mathbf{r}, [s : i - 1], \Gamma \rangle \models \varphi_1$, and $\langle \mathbf{r}, [i : i], \Gamma \rangle \models \varphi_2$

Figure 6: Formal semantics of our LTL system. The notation $\mathbf{r}[i]$ is used to fetch all the facts corresponding to time step i in \mathbf{r} , which contains in total m time steps. Γ represents a *variable grounding* that maps each quantified variable into a concrete entity in the database.

2. Evolving attribute of a single entity. E.g., $0.05 :: \text{deformed}(3, e)$ represents “an entity e is not deformed at time 3”. $0.92 :: \text{walk}(10, \text{MUGEN}, \text{right})$ stands for “MUGEN is walking to the right at time 10”.
3. Evolving relations of a pair of entities, e.g., $0.88 :: \text{next-to}(5, e_1, e_2)$ for “ e_1 is next to e_2 at time 5”.

Except for the static properties, others are relational facts that evolve over time, and thus contain the time step number. Note that our time step does not directly correspond to each frame. While there are other discretizations of time, in this work, each time step represents an ID of a clip, which is a size k sliding window of the video. We assume that the ST-SG is discretized into m time steps.

5.2. Spatio-Temporal Alignment Checking

Given a probabilistic database \mathbf{r} that encodes an ST-SG, and a specification ψ , we aim to measure the alignment score $\Pr(\mathbf{r} \models \psi)$ in an end-to-end and differentiable manner. Conceptually, each probabilistic fact in the database can be toggled on or off, resulting in $2^{|\mathbf{r}|}$ distinct *worlds*. Denoting each world as $w \in \mathcal{P}(\mathbf{r})$ ³, we can check whether the world w satisfies the specification ψ or not. From here, the alignment score can be computed as the sum of the probabilities of worlds satisfying ψ :

$$\Pr(\mathbf{r} \models \psi) = \sum_{w \in \mathcal{P}(\mathbf{r}), w \models \psi} \prod_{f \in w} \Pr(f), \quad (3)$$

In real life, enumerating all possible worlds is intractable. Existing general-purpose neuro-symbolic systems such as Scallop employ scalable algorithms to approximate this probability. We find the approximation helpful since it greatly reduces the time for probabilistic reasoning.

³ \mathcal{P} represents power-set.

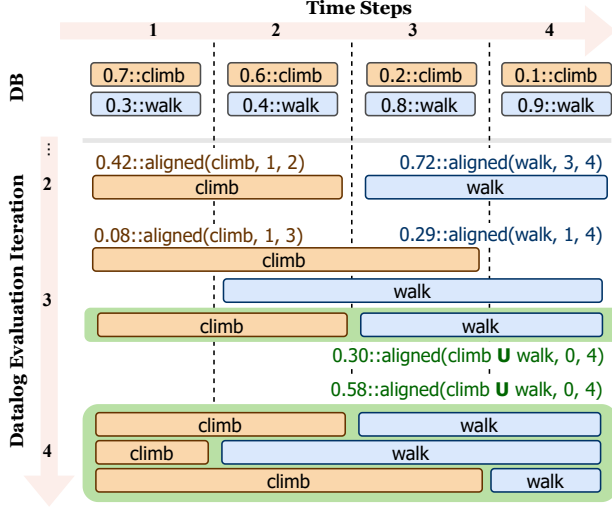


Figure 7: The evaluation process aligning a spatio-temporal scene graph (DB) with a specification `climb U walk`. In this example, we elide showing the arguments of the relational predicates and focus on matching sequential events.

LASER implements the spatio-temporal alignment checker using the Scallop system. This helps us to succinctly and precisely encode the formal semantics of LTL, which is defined in Figure 6. It inductively computes the alignment between a temporal slice of \mathbf{r} and an LTL formula. The whole specification ψ is aligned if the full \mathbf{r} (from 1 to m) satisfies ψ with a concrete variable grounding Γ . While we show the full alignment checker in the appendix, we illustrate one simplified evaluation process in Figure 7. Scallop’s Datalog engine iteratively aligns the predicted probabilistic events (simplified to just `climb` and `walk`) with the specification. At the 4th iteration, Scallop derives 3 different satisfying alignments. Aggregating them together gives the final alignment score 0.58.

5.3. Loss Function

Contrastive Learning. Unavoidable human biases exist in the specification, and contrastive learning can effectively reduce the bias and generate explanations of better quality. Let (X_i, ψ_i) and (X_j, ψ_j) be two datapoints in a mini-batch B , where ψ_i and ψ_j are the specifications for video X_i and X_j correspondingly. If $X_i \models \psi_j$, then it is an extra positive sample to the video X_i , else it is a negative sample to X_i . We can thus define our contrastive loss:

$$\mathcal{L}_c = \frac{1}{|B|^2} \sum_{(X_i, \psi_i) \in B} \sum_{(X_j, \psi_j) \in B} \mathcal{L}(\text{Pr}(M_\theta(X_i) \models \psi_j), \mathbb{1}[\psi_i = \psi_j]). \quad (4)$$

Note that, due to the one-to-many property existing in the specification-video pairs, it is possible to incorporate noises under the weak supervision setup, as the ground truth sym-

bolic representation of the video is not available to check against the specifications.

Time-Span Supervision. As our alignment checker provides not only the final query result but also the intermediate reasoning steps during the evaluation process, we can provide fine-grained supervision over the temporal dimension. A temporal loss can be devised for any subexpressions in which one has external knowledge of its time boundary.

Suppose a subexpression ψ' of the specification ψ should correspond to a time boundary (t_1, t_2) . Along with the final query result, we can also query for all possible time boundaries $\{(u_1, v_1), \dots, (u_n, v_n)\}$ where the subexpression ψ' is satisfied. The conditional alignment scores, $\text{Pr}(\hat{\mathbf{r}} \models \psi \mid \hat{\mathbf{r}}[u : v] \models \psi')$, are also deduced by the reasoning engine. Then we can weigh the loss according to the distance between (u, v) and (t_1, t_2) . Let d be the distance function and T be the time span length. Then, we have:

$$\mathcal{L}_t = \sum_{u \in T} \sum_{v \in T} d((u, v), (t_1, t_2)) \mathcal{L}(\text{Pr}(\hat{\mathbf{r}} \models \psi \mid \hat{\mathbf{r}}[u : v] \models \psi'), 1). \quad (5)$$

In practice, the loss function design is more flexible. In the 20BN dataset, we devised our temporal loss function based on the insight that the precondition should be satisfied near the beginning of the video, and the postcondition should be toward the end. We thus weigh the loss according to the difference between the two time stamps $|t_{\text{post}} - t_{\text{pre}}|$.

Semantic Loss. To provide further supervision, we resort to human knowledge encoded in the form of integrity constraints. We introduce semantic loss reflecting the probability of violating the integrity constraints. For example, an entity in a video cannot be `open` and `closed` at the same time; an entity that is not `bendable` cannot be `deformed`. These integrity constraints may interweave so heavily that it is hard to use a simple disjoint multi-class classifier to enforce. We encode all integrity constraints in the form of first-order logic rules, and our reasoning engine will also generate the probability that these constraints are violated. We thus have the semantic loss as an extra-weighted term after calculating the other loss components.

$$\mathcal{L}_s = \sum_{i=0}^n w_i \mathcal{L}(\text{Pr}(\hat{\mathbf{r}} \models \psi_{IC_i}), 0), \quad (6)$$

where n is the number of total integrity constraints, and w_i is a tunable parameter that specifies the weight of the integrity constraint ψ_{IC_i} in the total semantic loss.

6. Evaluation

We evaluate LASER on two datasets for video understanding: a realistic dataset 20BN-Something-Something and a synthetic dataset MUGEN. All experiments are conducted on a machine with two 20-core Intel Xeon CPUs, four GeForce RTX 2080 Ti GPUs, and 768 GB RAM.

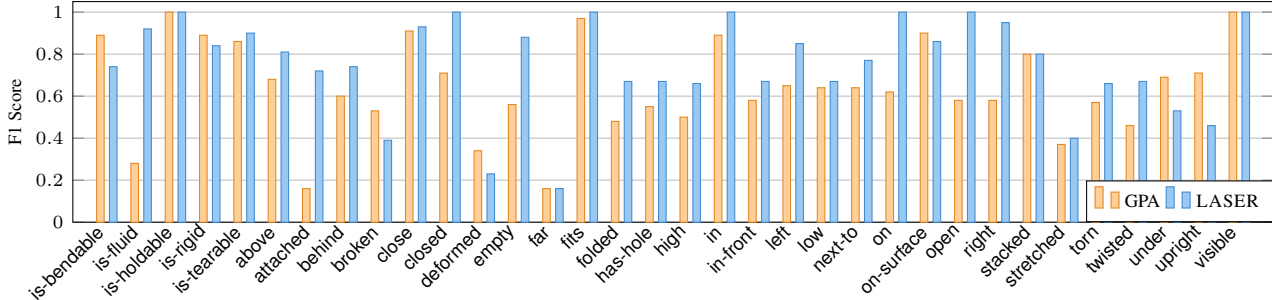


Figure 8: Per-predicate performance comparison against the GPA baseline using F1 metric. The arity of each predicate is denoted by “/n”. Our method outperforms the baseline on 79.4% of the predicates.

Dataset	Down-Stream Task	Baselines		LASER
20BN	ST-SG Prediction	GPA	0.74	0.78
MUGEN	Spec-Retrieval	SDSC	87.00%	90.12%
	Video-Retrieval		86.80%	88.10%

Table 1: Performance comparison to baselines on down-stream tasks. For the ST-SG prediction task, performance is evaluated using the F1 metric.

6.1. 20BN-Something-Something

Dataset. The 20BN dataset consists of (a) video and action pairs of humans performing everyday actions with ordinary objects [14], (b) expert designed preconditions and postconditions for the actions in the PDDL language [33], and (c) frame-based object bounding boxes [31]. There are 172 actions with 37 underlying predicates in this dataset. Specifically, there are 6 static predicates, 21 unary predicates, and 10 binary predicates. The static predicates represent object attributes that persist over time; the unary predicates reflect a single object’s state; the binary predicates reflect the relationship between two objects. We train on 10,000 training datapoints and test on 1000, where the training and testing splits follow the 20BN-Something-Something dataset.

Temporal Specifications. We build the temporal specifications for each action on top of the given PDDL specifications. The PDDL specification is composed of a precondition and a postcondition which are propositional logic formulas over constants representing object names, and free variables with regard to object IDs. We thus define the high-level temporal specifications for actions as $\Diamond(\psi_{\text{pre}} \wedge \Diamond\psi_{\text{post}})$. We implement a parser that takes in the PDDL specification and generates the temporal specification in Scallop.

Experimental Setup. As the ground truth symbolic representation of the whole video is not accessible, we use the same heuristic quantitative evaluation metric as the baseline. We assert that the precondition holds at the first frame, and the postcondition holds at the last frame. During test time, the neural model predicts the symbolic representations

of the first and last images of the video and checks against the precondition and postcondition. F1-score is used to evaluate the recognition quality of each fine-grained predicate. Since the evaluation metric requires frame-based symbolic video representation, we set the video clip size to 1.

We use a convolutional model for the frame features, an ROI Pooler for object features, an LSTM model for video-wise object embeddings, and MLP layers for predicate output distributions. We adopt temporal supervision loss with the prior that the precondition and postcondition should be far away from each other; contrastive learning loss with batch size 3; and semantic loss with a weight of 0.05, where the integrity constraints, such as “a rigid object is not fluid”, are obtained from the original PDDL file. More training details are included in the appendix.

Quantitative Study. We compare against GPA [33], a DNF cross-entropy loss based approach. GPA uses heuristics to obtain the two frames which satisfy the pre- and post-conditions from a video, while LASER uses a generic temporal specification. As shown in Table 1, we achieve a higher average F1-score than the baseline. On the fine-grained predicates Figure 8, our model performs better than the baseline on around 79.4% of the predicates.

Qualitative Study. We showcase the trained model’s frame-wise predictions on a few testing datapoints in Figure 9. Though only weak supervision is provided, our model can learn the fine-grained representations and thus explain the reasoning process of why the video is corresponding to the given specification.

6.2. MUGEN

Dataset. MUGEN [16] is a synthetic dataset that is based on an open-sourced platform game CoinRun [8]. Each datapoint contains a 3.2s video snippet of the gameplay and a corresponding automatically generated text describing the video. The agent in the game can perform 6 actions: walk, jump, kill, collect, die, and climb. There are 13 different characters and entities in the game, including various enemies and collectibles. A video may

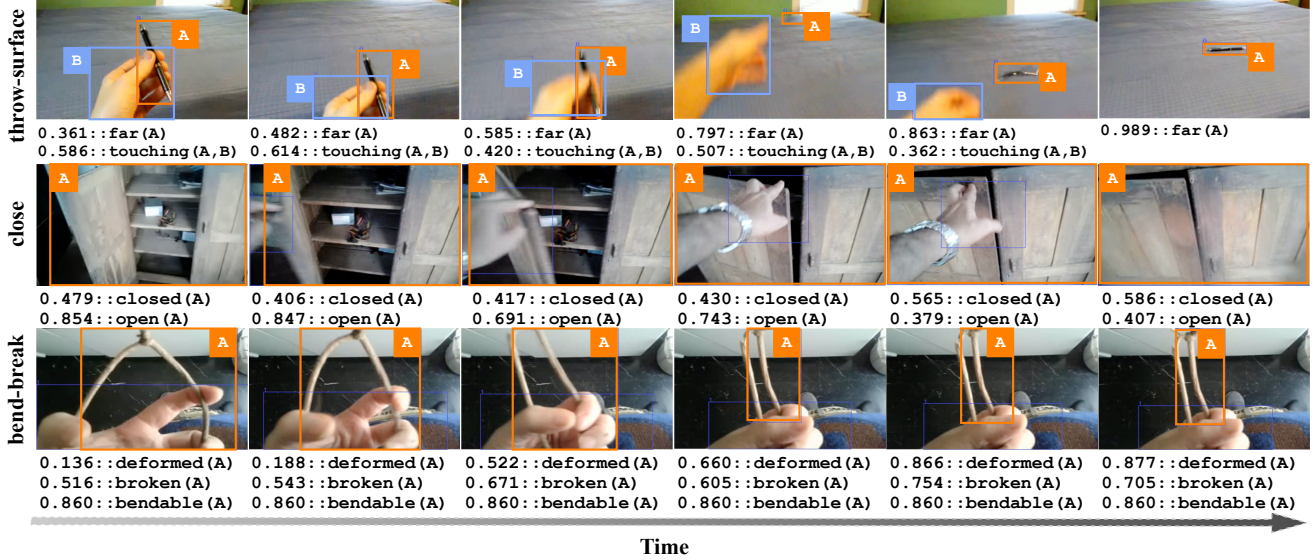


Figure 9: The ST-SGs predicted by LASER on the 20BN dataset. The high-level actions are labeled on the left.

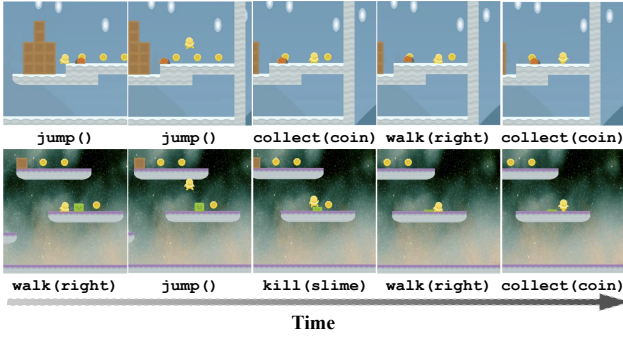


Figure 10: Examples of the predicted MUGEN actions predicted. We elide showing M in each predicate for brevity.

contain any sequence of actions, which may be simple or complex. We train on 5,000 training datapoints and test on 1,000 datapoints, where the training and testing splits are already provided in the dataset.

Temporal Specifications. We construct the temporal specification from the given text description using a simple heuristic-based semantic parser. We first extract an ordered action list $[a_1, a_2, \dots, a_n]$ from the text with heuristics, then construct the temporal specification as $a_1 \cup a_2 \dots \cup a_n$. This specification means the actions are performed one by one with no intermediate gaps.

Experimental Setup. We evaluate our approach on a downstream video-specification retrieval task. Given three videos and three specifications, we want to match the correctly aligned pair together. Specifically, we evaluate the accuracy with which we infer whether the correct specification has the highest alignment score, and vice versa, given the video. We denote the two tasks as spec-retrieval and

video-retrieval respectively.

The neural perception model consists of an S3D video encoding model pretrained on Kinetics 400 [21], and MLP layers to classify the actions. The video is first passed through the S3D [41] model for frame-based embeddings. Then all the embeddings that occur in a video clip are concatenated as the input to a 2-layer MLP classifier. We set the number of frames per clip to 2. The classifier thus produces clip-wise video representations. We employ contrastive loss and semantic loss for training.

Quantitative Study. As shown in Table 1, LASER outperforms the SDSC baseline [16], an embedding-based approach presented along with the MUGEN dataset. SDSC learns a projection from video and text embeddings to a joint embedding space and uses a scaled cosine distance function to measure the similarity. SDSC utilizes the same pre-trained video embedding model S3D and DistilBERT [38] for specification embeddings. Compared to the baseline, LASER achieves better performance on both specification and video retrieval tasks.

Qualitative Study. LASER provides clip-level explanations along with the retrieval results. We illustrate the fine-grained model predictions on two test datapoints in Figure 10. Our approach can even identify actions that persist for a very short period of time, such as `kill` an enemy.

7. Conclusion and Future Outlook

We present LASER, a neuro-symbolic approach for learning semantic video representations. Our approach captures the rich spatial and temporal properties of a video by learning a spatio-temporal scene graph through weak supervision in the form of linear temporal logic specifications.

We evaluate our work on two datasets 20BN-Something-Something and MUGEN which exhibit diverse temporal properties. LASER outperforms the current baselines on downstream tasks while providing explainability.

The current limitations of LASER include the requirement for pre-specifying the relational schema and providing complex temporal specifications. In the future, we plan to extend our approach by incorporating the natural language modality into our end-to-end pipeline, i.e., learning to systematically extract the schema and the spatio-temporal specifications from natural language captions and common-sense knowledge bases.

References

- [1] Susanne Albers, Alberto Marchetti-Spaccamela, Yossi Matias, Sotiris Nikolettseas, and Wolfgang Thomas. *Automata, Languages and Programming: 36th International Colloquium, ICALP 2009, Rhodes, Greece, July 5-12, 2009, Proceedings, Part I*, volume 5555. Springer Science & Business Media, 2009. 4
- [2] Saeed Amizadeh, Hamid Palangi, Alex Polozov, Yichen Huang, and Kazuhito Koishida. Neuro-symbolic visual reasoning: Disentangling. In *International Conference on Machine Learning*, pages 279–290. PMLR, 2020. 3
- [3] Max Bain, Arsha Nagrani, Gül Varol, and Andrew Zisserman. Frozen in time: A joint video and image encoder for end-to-end retrieval. In *Proceedings of the IEEE/CVF International Conference on Computer Vision*, pages 1728–1738, 2021. 2
- [4] Gertjan J. Burghouts, Fieke Hillerström, Erwin Walraven, Michael van Bekkum, Frank Ruis, and Joris Sijs. Anomaly detection in an open world by a neuro-symbolic program on zero-shot symbols. In *IROS 2022 Workshop Probabilistic Robotics in the Age of Deep Learning*, 2022. 4
- [5] Sagar Chaki, Edmund Clarke, Joël Ouaknine, Natasha Sharygina, and Nishant Sinha. Concurrent software verification with states, events, and deadlocks. *Formal Aspects of Computing*, 17(4):461–483, 2005. 4
- [6] Chien-Yi Chang, De-An Huang, Yanan Sui, Li Fei-Fei, and Juan Carlos Nieves. D3tw: Discriminative differentiable dynamic time warping for weakly supervised action alignment and segmentation. In *Proceedings of the IEEE/CVF Conference on Computer Vision and Pattern Recognition*, pages 3546–3555, 2019. 3
- [7] Zhenfang Chen, Kexin Yi, Yunzhu Li, Mingyu Ding, Antonio Torralba, Joshua B Tenenbaum, and Chuang Gan. Comphy: Compositional physical reasoning of objects and events from videos. *arXiv preprint arXiv:2205.01089*, 2022. 3
- [8] Karl Cobbe, Oleg Klimov, Chris Hesse, Taehoon Kim, and John Schulman. Quantifying generalization in reinforcement learning. In *International Conference on Machine Learning*, pages 1282–1289. PMLR, 2019. 7
- [9] Luc De Raedt, Angelika Kimmig, and Hannu Toivonen. Problog: A probabilistic prolog and its application in link discovery. In *IJCAI*, volume 7, pages 2462–2467. Hyderabad, 2007. 4
- [10] Li Ding and Chenliang Xu. Weakly-supervised action segmentation with iterative soft boundary assignment. In *Proceedings of the IEEE conference on computer vision and pattern recognition*, pages 6508–6516, 2018. 3
- [11] Xuchu Ding, Stephen L Smith, Calin Belta, and Daniela Rus. Optimal control of markov decision processes with linear temporal logic constraints. *IEEE Transactions on Automatic Control*, 59(5):1244–1257, 2014. 4
- [12] Nikita Dvornik, Isma Hadji, Konstantinos G. Derpanis, Animesh Garg, and Allan D. Jepson. Drop-dtw: Aligning common signal between sequences while dropping outliers. *CoRR*, abs/2108.11996, 2021. 3
- [13] Debidatta Dwivedi, Yusuf Aytar, Jonathan Tompson, Pierre Sermanet, and Andrew Zisserman. Temporal cycle-consistency learning. *CoRR*, abs/1904.07846, 2019. 3
- [14] Raghav Goyal, Samira Ebrahimi Kahou, Vincent Michalski, Joanna Materzynska, Susanne Westphal, Heuna Kim, Valentin Haenel, Ingo Fründ, Peter Yianilos, Moritz Mueller-Freitag, Florian Hoppe, Christian Thureau, Ingo Bax, and Roland Memisevic. The “something something” video database for learning and evaluating visual common sense. *CoRR*, abs/1706.04261, 2017. 2, 3, 7
- [15] Tengda Han, Weidi Xie, and Andrew Zisserman. Temporal alignment networks for long-term video. In *Proceedings of the IEEE/CVF Conference on Computer Vision and Pattern Recognition*, pages 2906–2916, 2022. 2, 3
- [16] Thomas Hayes, Songyang Zhang, Xi Yin, Guan Pang, Sasha Sheng, Harry Yang, Songwei Ge, Qiyuan Hu, and Devi Parikh. MUGEN: A playground for video-audio-text multimodal understanding and generation. 2, 3, 7, 8
- [17] Pascal Hitzler. Neuro-symbolic artificial intelligence: The state of the art. 2022. 3
- [18] De-An Huang, Li Fei-Fei, and Juan Carlos Nieves. Connectionist temporal modeling for weakly supervised action labeling. In *Computer Vision—ECCV 2016: 14th European Conference, Amsterdam, The Netherlands, October 11–14, 2016, Proceedings, Part IV 14*, pages 137–153. Springer, 2016. 3
- [19] Jiani Huang, Ziyang Li, Binghong Chen, Karan Samel, Mayur Naik, Le Song, and Xujie Si. Scallop: From probabilistic deductive databases to scalable differentiable reasoning. *Advances in Neural Information Processing Systems*, 34:25134–25145, 2021. 2, 3, 4
- [20] Chao Jia, Yinfei Yang, Ye Xia, Yi-Ting Chen, Zarana Parekh, Hieu Pham, Quoc V. Le, Yun-Hsuan Sung, Zhen Li, and Tom Duerig. Scaling up visual and vision-language representation learning with noisy text supervision. *CoRR*, abs/2102.05918, 2021. 2
- [21] Will Kay, Joao Carreira, Karen Simonyan, Brian Zhang, Chloe Hillier, Sudheendra Vijayanarasimhan, Fabio Viola, Tim Green, Trevor Back, Paul Natsev, et al. The kinetics human action video dataset. *arXiv preprint arXiv:1705.06950*, 2017. 8
- [22] Yonit Kesten, Amir Pnueli, and Li-on Raviv. Algorithmic verification of linear temporal logic specifications. In *Automata, Languages and Programming: 25th International Colloquium, ICALP’98 Aalborg, Denmark, July 13–17, 1998 Proceedings 25*, pages 1–16. Springer, 1998. 4

- [23] Alina Kuznetsova, Hassan Rom, Neil Alldrin, Jasper R. R. Uijlings, Ivan Krasin, Jordi Pont-Tuset, Shahab Kamali, Stefan Popov, Matteo Mallocci, Tom Duerig, and Vittorio Ferrari. The open images dataset V4: unified image classification, object detection, and visual relationship detection at scale. *CoRR*, abs/1811.00982, 2018. 1
- [24] Gen Li, Nan Duan, Yuejian Fang, Daxin Jiang, and Ming Zhou. Unicoder-vl: A universal encoder for vision and language by cross-modal pre-training. *CoRR*, abs/1908.06066, 2019. 2
- [25] Junnan Li, Ramprasaath R. Selvaraju, Akhilesh Deepak Gotmare, Shafiq R. Joty, Caiming Xiong, and Steven C. H. Hoi. Align before fuse: Vision and language representation learning with momentum distillation. *CoRR*, abs/2107.07651, 2021. 2
- [26] Qing Li, Siyuan Huang, Yining Hong, Yixin Chen, Ying Nian Wu, and Song-Chun Zhu. Closed loop neural-symbolic learning via integrating neural perception, grammar parsing, and symbolic reasoning. In *International Conference on Machine Learning*, pages 5884–5894. PMLR, 2020. 2, 4
- [27] Cewu Lu, Ranjay Krishna, Michael S. Bernstein, and Li Fei-Fei. Visual relationship detection with language priors. *CoRR*, abs/1608.00187, 2016. 1
- [28] Jiasen Lu, Vedanuj Goswami, Marcus Rohrbach, Devi Parikh, and Stefan Lee. 12-in-1: Multi-task vision and language representation learning. *CoRR*, abs/1912.02315, 2019. 2
- [29] Robin Manhaeve, Sebastijan Dumancic, Angelika Kimmig, Thomas Demeester, and Luc De Raedt. Deepproblog: Neural probabilistic logic programming. *CoRR*, abs/1805.10872, 2018. 2, 3, 4
- [30] Jiayuan Mao, Chuang Gan, Pushmeet Kohli, Joshua B. Tenenbaum, and Jiajun Wu. The Neuro-Symbolic Concept Learner: Interpreting Scenes, Words, and Sentences From Natural Supervision. In *International Conference on Learning Representations*, 2019. 3, 4
- [31] Joanna Materzynska, Tete Xiao, Roei Herzig, Huijuan Xu, Xiaolong Wang, and Trevor Darrell. Something-else: Compositional action recognition with spatial-temporal interaction networks. In *Proceedings of the IEEE/CVF Conference on Computer Vision and Pattern Recognition*, pages 1049–1059, 2020. 7
- [32] Antoine Miech, Jean-Baptiste Alayrac, Lucas Smaira, Ivan Laptev, Josef Sivic, and Andrew Zisserman. End-to-end learning of visual representations from uncurated instructional videos. *CoRR*, abs/1912.06430, 2019. 2
- [33] Toki Migimatsu and Jeannette Bohg. Grounding predicates through actions. In *2022 International Conference on Robotics and Automation (ICRA)*, pages 3498–3504. IEEE, 2022. 7, 11
- [34] Amir Pnueli. The temporal logic of programs. *18th Annual Symposium on Foundations of Computer Science (sfcs 1977)*, pages 46–57, 1977. 2, 4
- [35] Alec Radford, Jong Wook Kim, Chris Hallacy, Aditya Ramesh, Gabriel Goh, Sandhini Agarwal, Girish Sastry, Amanda Askell, Pamela Mishkin, Jack Clark, et al. Learning transferable visual models from natural language supervision. In *International conference on machine learning*, pages 8748–8763. PMLR, 2021. 2
- [36] Alexander Richard, Hilde Kuehne, Ahsan Iqbal, and Juer-gen Gall. Neuralnetwork-viterbi: A framework for weakly supervised video learning. In *Proceedings of the IEEE conference on Computer Vision and Pattern Recognition*, pages 7386–7395, 2018. 3
- [37] Dorsa Sadigh, Eric S Kim, Samuel Coogan, S Shankar Sastry, and Sanjit A Seshia. A learning based approach to control synthesis of markov decision processes for linear temporal logic specifications. In *53rd IEEE Conference on Decision and Control*, pages 1091–1096. IEEE, 2014. 4
- [38] Victor Sanh, Lysandre Debut, Julien Chaumond, and Thomas Wolf. Distilbert, a distilled version of bert: smaller, faster, cheaper and lighter. *arXiv preprint arXiv:1910.01108*, 2019. 8
- [39] Xindi Shang, Tongwei Ren, Jingfan Guo, Hanwang Zhang, and Tat-Seng Chua. Video visual relation detection. In *Proceedings of the 25th ACM international conference on Multimedia*, pages 1300–1308, 2017. 1
- [40] Thomas Winters, Giuseppe Marra, Robin Manhaeve, and Luc De Raedt. Deepstochlog: Neural stochastic logic programming. *CoRR*, abs/2106.12574, 2021. 2, 3, 4
- [41] Saining Xie, Chen Sun, Jonathan Huang, Zhuowen Tu, and Kevin Murphy. Rethinking spatiotemporal feature learning: Speed-accuracy trade-offs in video classification. In *Proceedings of the European conference on computer vision (ECCV)*, pages 305–321, 2018. 8
- [42] Hu Xu, Gargi Ghosh, Po-Yao Huang, Dmytro Okhonko, Armen Aghajanyan, Florian Metze, Luke Zettlemoyer, and Christoph Feichtenhofer. Videoclip: Contrastive pre-training for zero-shot video-text understanding. *arXiv preprint arXiv:2109.14084*, 2021. 2
- [43] Ziwei Xu, Yogesh S Rawat, Yongkang Wong, Mohan Kankanhalli, and Mubarak Shah. Don’t pour cereal into coffee: Differentiable temporal logic for temporal action segmentation. In Alice H. Oh, Alekh Agarwal, Danielle Belgrave, and Kyunghyun Cho, editors, *Advances in Neural Information Processing Systems*, 2022. 3
- [44] Hanlin Zhang, Ziyang Li, Jiani Huang, Mayur Naik, and Eric Xing. Improved logical reasoning of language models via differentiable symbolic programming. In *First Workshop on Pre-training: Perspectives, Pitfalls, and Paths Forward at ICML 2022*, 2022. 4
- [45] Guangming Zhu, Liang Zhang, Youliang Jiang, Yixuan Dang, Haoran Hou, Peiyi Shen, Mingtao Feng, Xia Zhao, Qiguang Miao, Syed Afaq Ali Shah, et al. Scene graph generation: A comprehensive survey. *arXiv preprint arXiv:2201.00443*, 2022. 1

A. MUGEN

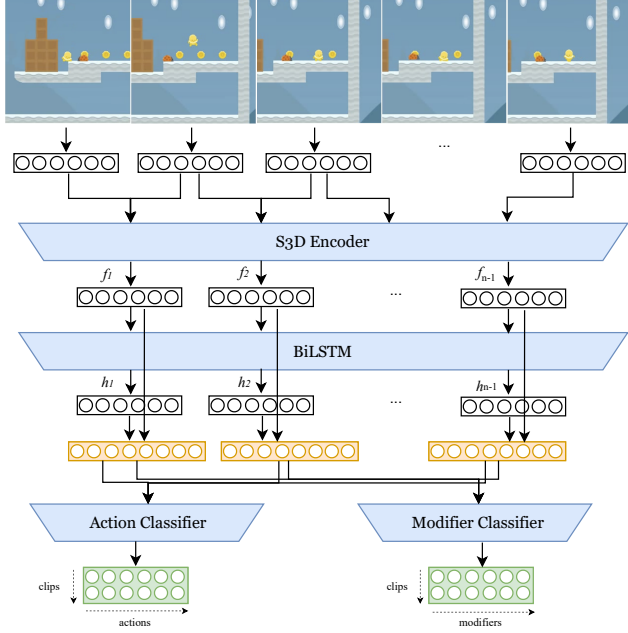


Figure 11: MUGEN model architecture.

Model Architecture We present the model architecture overview in Figure 11. The video is first segmented into clips through a sliding window of length 2. Then, each clip is encoded through an S3D model and yields clip-wise embedding. The embedding is further passed into a BiLSTM model to obtain the context for each clip. An action classifier takes in the concatenation of the clip-based embedding and its context embedding, and classifies each clip into 6 actions: walk, jump, kill, collect, die, and climb. Further, a modifier classifier predicts the 4 possible direction of the actions: left, right, up, down. The matching process of action and its modifier is also performed in the reasoner. For example, a combination of collect, left will be invalidated during reasoning.

Learning Setup We train the model on 5000 training datapoints, and 1000 test datapoints. The contrastive loss is obtained over a batch size 3; the violation loss is constructed with regard to the axioms in GPA [33]. We train the model with a learning rate of 0.0001, violation weight 0.01, number of epochs 100, and batch size 3. The Scallop reasoning engine setup is using difftopkproofs provenance with k set to 5.

B. 20BN-Something-Something.

Model Architecture We use a 4-layer convolutional model to extract the features for each frame and a ROIpooler to obtain the embedding for each object on the

frame. To obtain the static predicates, we pass the frame-wise object embeddings through an LSTM encoder to obtain the video-wise object embedding, and a 2-layer MLP classifier yields the output distribution. For the unary predicates, a 2-layer MLP classifier takes in the concatenation of the frame embedding, object embedding, and the object bounding box, and generates the output distribution. For the binary predicates, a 3-layer MLP classifier takes in the concatenation of the frame embedding, two object embeddings, and two object bounding boxes, and generates the output distribution. The overview of the architecture is shown in Figure 5.

Temporal Loss Function. We showcase the temporal loss design for the 20bn-something-something dataset, whose temporal logic specification $\psi = \Diamond(\psi_{\text{pre}} \wedge \Diamond\psi_{\text{post}})$, where ψ_{pre} is precondition and ψ_{post} is postcondition. Given the prior knowledge that the video contains only one action, the ground truth clip that corresponds to the precondition shall be near the beginning of the video, while the clip satisfying the post-condition shall be toward the end of the video. By executing ψ with the symbolic database \hat{r} , we can obtain all possible time spans d between pairs of video clips where the precondition and post are satisfied and their corresponding alignment score with the specification s . The larger the d is, the more likely the two clips are actually satisfying the pre-condition and post-conditions, rather than being a noisy signal. To represent this intuition, we first design a weight function using thresholded linear interpolation with regard to distance. Let the maximum possible distance between any pair of clips be d_{max} , and the minimum threshold for the distance be d_{τ} .

$$w_d = \begin{cases} 0 & \text{if } d \leq d_{\tau} \\ \frac{d-d_{\tau}}{d_{\text{max}}-d_{\tau}} & \text{if } d > d_{\tau} \end{cases}$$

Instead of using just querying for the alignment score $s_{\mathbf{r}}^{\psi}$, we instead query for the conditional alignment score $s_d = Pr(s_{\mathbf{r}}^{\psi} | d)$ which is conditioned on the distance d between ψ_{pre} and ψ_{post} are satisfied. To incorporate our temporal supervision by biasing toward longer distance supervision, we re-weight the conditional alignment scores using the weight function above.

$$\mathcal{L}_t = \sum_{d=0}^{d_{\text{max}}} w_d \mathcal{L}(s_d, 1)$$

In the experiment, we set the threshold d_{τ} to be $0.9d_{\text{max}}$.

Learning Setup. The contrastive loss is obtained over a batch size 3; the violation loss is constructed with regard to the axioms in GPA [33]. We train the model with a learning rate of 0.0001, violation weight 0.05, number of epochs 50, and batch size 3. The Scallop reasoning engine setup is using difftopkproofs provenance with $k=3$.




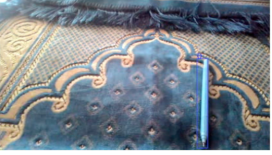
Frame	0	10	20	30
Video: pull right				
temporal	1.000: left(A) 1.000: right(A)	1.000: left(A) 1.000: right(A)	1.000: left(A) 1.000: right(A)	1.000: left(A) 1.000: right(A)
temporal + contrastive	0.950: left(A) 0.318: right(A)	0.732: left(A) 0.484: right(A)	0.991: left(A) 0.827: right(A)	0.912: left(A) 0.657: right(A)
temporal + contrastive + violation	0.302: left(A) 0.587: right(A)	0.196: left(A) 0.660: right(A)	0.236: left(A) 0.819: right(A)	0.032: left(A) 0.994: right(A)

Figure 12: Comparing model performance trained with different loss functions.

```

// Datalog implementation for fact matching
eval(psi, fid, fid + 1) :- pred(psi, p), frame(fid, p)
eval(psi, start_fid, end_fid + 1) :- eval(psi, start_fid, end_fid), pred(psi, p), frame(end_fid, p)

// Datalog implementation for until
eval(psi, start_fid, end_fid) :- until_expr(psi, psi_1, psi_2),
    eval(psi_1, start_fid, mid_fid), eval(psi_2, mid_fid + 1, end_fid)

// Datalog implementation for finally
eval(psi, start_fid_1, end_fid_2) = finally_expr(psi, psi_1, psi_2),
    eval(psi_1, start_fid_1, end_fid_1), eval(psi_2, start_fid_2, end_fid_2),
    start_fid_1 < start_fid_2

// Datalog implementation for next
eval(psi, start_fid, end_fid) = next_expr(psi, psi_1, psi_2),
    eval(psi_1, start_fid, end_fid - 1), eval(psi_2, end_fid - 1, end_fid)

// Datalog implementation for global
eval(psi, start_fid, end_fid) = global_expr(psi, psi_1), eval(psi_1, start_fid, end_fid)

```

Figure 13: One implementation of linear temporal logic (LTL) using Datalog.

Ablation Studies. We study how different loss impact the qualitative evaluation result, as shown in Figure 12. In this task, the spatiotemporal specifications are manually crafted, which also means a lot of biases are introduced. As we can see, using only temporal loss yields us a counter-intuitive result, a 1.00 probability for both the object on the left of the camera and on the right of the camera. This is mainly due to the imbalanced low-level supervision that is introduced by human bias. By adding a contrastive loss, we can see an improvement in that the model predicts the ground truth position with a higher probability compared to its counterpart. Incorporating a violation loss can further improve the performance in that the sum of the probabilities

is closer to 1.0.

C. Temporal Reasoner

We showcase one temporal reasoner design in this section that enables all linear temporal language features: \square , \diamond , \bigcirc , and \mathbf{U} in Figure 13. Note that we only lay out the core matching process of LTL, while the reasoner can be configured and extended with all other Datalog features, such as grounding free variables.